

Guilherme Paula Pinto Schettino
Mauro Roberto Tucci
Rogério Sousa
Carmen Silvia Valente Barbas
Marcelo Britto Passos Amato
Carlos Roberto Ribeiro Carvalho

Mask mechanics and leak dynamics during noninvasive pressure support ventilation: a bench study

Received: 11 June 2001
Final revision received: 15 September 2001
Accepted: 26 September 2001
Published online: 10 November 2001
© Springer-Verlag 2001

Supported by FAPESP and LIM-FMUSP, Brazil.

G. P. P. Schettino · M. R. Tucci · R. Sousa ·
C. S. V. Barbas · M. B. P. Amato ·
C. R. R. Carvalho (✉)
Experimental Laboratory of Mechanical
Ventilation, Respiratory ICU,
Pulmonary Division,
Hospital das Clínicas and Heart Institute,
University of São Paulo Medical School,
São Paulo, Brazil
E-mail: crrcarvalho@uol.com.br

C. R. R. Carvalho
Rua Maria Figueiredo 396 Apt. 141,
São Paulo, SP, CEP 04002-002, Brazil

Introduction

A mask, or an equivalent device providing connection between patient and ventilator, and the associated air leak around the mask are the principal differences between noninvasive positive pressure ventilation (NPPV) and the standard invasive ventilatory approach. However, little information is available on mask mechanics and air leak dynamics during NPPV [1, 2, 3]. The use of a thigh mask causes patient discomfort and may lead to skin breakdown [4]. A massive air leak

Abstract Objective: To study the mask mechanics and air leak dynamics during noninvasive pressure support ventilation.

Setting: Laboratory of a university hospital.

Design: A facial mask was connected to a mannequin head that was part of a mechanical respiratory system model. The mask fit pressure ($P_{\text{mask-fit}}$) measured inside the mask's pneumatic cushion was adjusted to 25 cmH₂O using elastic straps. Pressure support (PS) was set to ensure a maximal tidal volume distal to the mask (VT_{distal}) but avoiding failure to cycle to exhalation.

Measurements: Airway pressure (P_{aw}), $P_{\text{mask-fit}}$, mask occlusion pressure ($P_{\text{mask-occl}} = P_{\text{mask-fit}} - P_{\text{aw}}$), VT_{proximal} (VT_{prox}), distal to the mask (VT_{distal}), air leak volume ($Leak = VT_{\text{prox}} - VT_{\text{distal}}$), and inspiratory air leak flow rate (difference between inspiratory flow proximal and distal to the mask) were recorded.

Results: PS 15 cmH₂O was the highest level that could be used without failure to cycle to exhalation (VT_{distal} of 585 ± 4 ml, leak of 32 ± 1 ml or $5.2 \pm 0.2\%$ of VT_{prox} , and a minimum $P_{\text{mask-occl}}$ of 1.7 ± 0.1 cmH₂O). During PS 16 cmH₂O the $P_{\text{mask-occl}}$ dropped to 1.1 ± 0.1 cmH₂O, and at this point all flow delivered by the ventilator leaked around the mask, preventing the inspiratory flow delivered by the ventilator from reaching the expiratory trigger threshold.

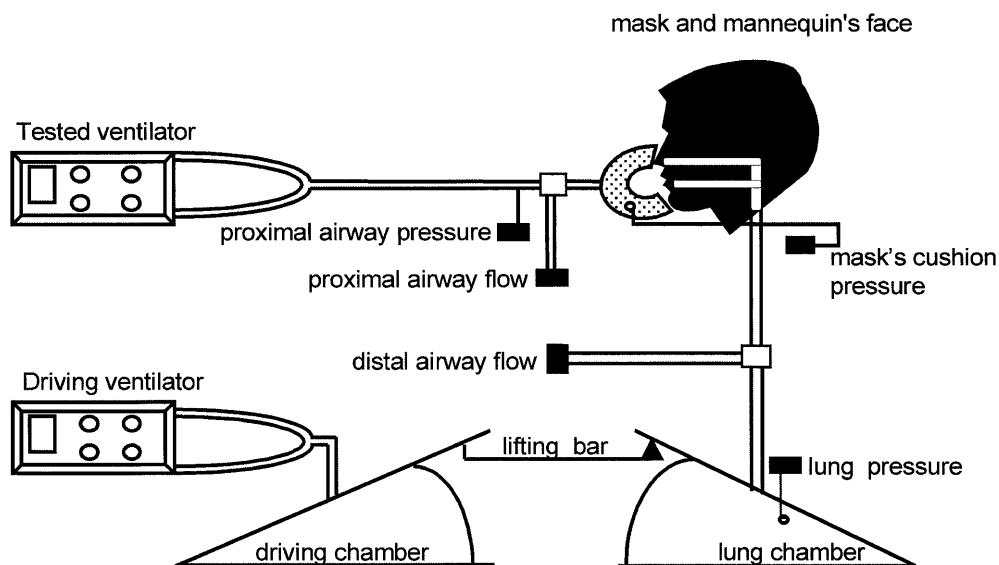
Conclusion: $P_{\text{mask-fit}}$ and $P_{\text{mask-occl}}$ can be easily measured in pneumatic cushioned masks and the data obtained may be useful to guide mask fit and inspiratory pressure set during noninvasive positive pressure ventilation.

Keywords Noninvasive positive pressure ventilation · Facial mask · Mask mechanics · Air leak

from the mask reduces alveolar ventilation and may lessen the efficacy of NPPV decreasing the breathing effort [5], and particularly during the use of pressure support ventilation (PS) air leak may interfere with patient-ventilator synchrony and ventilator operation [6].

We developed a mask fit respiratory system model that allowed the study of mask mechanics and air leak dynamics during simulation of noninvasive pressure support ventilation.

Fig. 1 Illustration of the experimental setup. The inspiratory effort was simulated using a two-chamber test lung model (TTL1600, Michigan Instruments, Grand Rapids, Mich., USA). The driving chamber was powered by an ICU ventilator (driving ventilator) set as follows: VT of 400 ml, sinusoidal inspiratory flow pattern at a peak flow of 1.5 l per second, and rate of 10 breaths/min. A metal lifting bar connected the driving and the lung chambers lifting the lung chamber with each breath of the driving ventilator. The lung chamber could inflate freely beyond by the VT delivered by the tested ventilator



Methods

Mask fit respiratory system model

The respiratory system model included a mannequin fiberglass head and a mechanical lung model (Fig. 1). A facial mask (Dryden Clear Comfort, adult-medium size, Gibeck, Indianapolis, Ind., USA) with an inflatable low-pressure air cushion was used during the experiment. The mask's cushion was inflated with 50 ml air. The pressure inside the cushion was less than 1 cmH₂O when it was inflated with this volume and disconnected from the model. The mask was fitted to the mannequin's face using an elastic headgear (Vital Sign, Totowa, N.J., USA). One pressure transducer (± 100 cmH₂O Validyne, Northridge, Calif., USA) was connected to the cushion's inflation valve to measure the pressure inside the cushion, which represented the pressure that fitted the mask against the mannequin's face [$P_{\text{mask-fit}}$ (cmH₂O)]. Prior to the application of PS the elastic straps tension were adjusted to obtain a $P_{\text{mask-fit}}$ of 25 cmH₂O.

Inspiratory efforts were simulated using a two-chamber lung as described by Op't Holt and associates [7]. The lung chamber (LC) compliance was set at 40 ml/cmH₂O and airway resistance at 5 cmH₂O/l per second. PS level (Evita IV, Drägerwerk, Germany) was set to ventilate the LC (VT_{distal}) with the greatest possible volume, but avoiding failure to cycle to exhalation. No positive end-expiratory pressure (PEEP) was applied.

Data acquisition and measured parameters

One pneumotachometer (Hans-Rudolph, Kansas City, Mo., USA) connected to a differential pressure transducer (± 2 cmH₂O, Validyne) and one differential pressure transducer (± 100 cmH₂O, Validyne) were placed between the Y connector of the tested ventilator and the mask to measure the proximal airway flow and pressure (P_{aw} ; Fig. 1). An additional pneumotachometer was positioned between the mannequin's upper airway and LC to measure the distal airway flow. The analog signals from these differential pressure transducers were amplified-digitized (PCI-Mio-16XE-50, National Instruments, Austin, Tex., USA) and recorded at 200 Hz using a

data acquisition system (Lab-View Software, National Instruments) for off-line analysis. Ten consecutive breaths were analyzed and the results reported as mean \pm SD.

The following parameters were analyzed: time integration of proximal and distal inspiratory flow (VT_{prox} and VT_{distal} , respectively). The air leak flow rate around the mask was defined as the difference between proximal and distal inspiratory flow, and the inspiratory leak volume was calculated by the difference between VT_{prox} and VT_{distal} ($Leak = VT_{\text{prox}} - VT_{\text{distal}}$). The gradient between $P_{\text{mask-fit}}$ and P_{aw} was electronically calculated and termed mask occlusion pressure ($P_{\text{mask-occl}} = P_{\text{mask-fit}} - P_{\text{aw}}$).

Results

In all recorded breaths the lung chamber was uncoupled from the driving chamber at the end of inspiration showing that VT_{distal} was delivered by the tested ventilator and not by the driving ventilator. PS 15 cmH₂O was the highest level that could be used without massive air leak and allowing the proximal flow to decline to the expiratory trigger threshold (25% of the peak inspiratory flow, i.e., about 0.30 l per second in this set). Inspiration ended by flow criteria in all analyzed breaths (Fig. 2). A VT_{distal} of 585 ± 4 ml was generated with a leak of 32 ± 1 ml or $5.2 \pm 0.2\%$ of the VT_{prox} . The lowest $P_{\text{mask-occl}}$ recorded during PS 15 was 1.7 ± 0.1 cmH₂O.

When PS 16 cmH₂O was tested a greater VT_{distal} (625 ± 3 ml) was achieved, but with a massive air leak around the mask (leak = 1170 ± 31 ml or $65.2 \pm 0.6\%$ of the VT_{prox}). The lowest recorded $P_{\text{mask-occl}}$ was 1.1 ± 0.1 cmH₂O and at this point the leak rate was about 0.39 l per second which prevented the proximal inspiratory flow from reaching the expiratory trigger threshold. Inspiration was ended by time norm since 4 s had passed (Fig. 2). The $P_{\text{mask-occl}}$ vs. leak rate curve re-

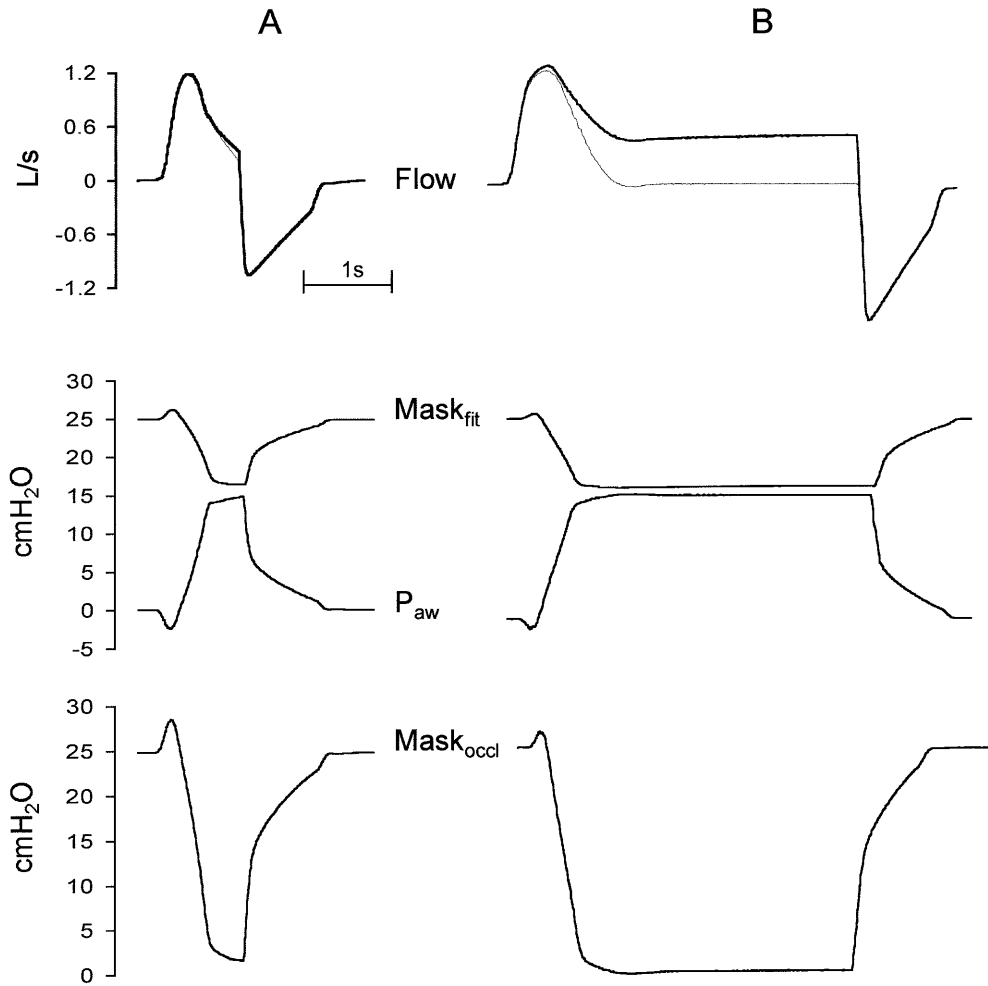


Fig. 2 **A** From top to bottom proximal (thick line) and distal to the mask flow tracings (thin line); mask fit pressure ($P_{mask-fit}$) and airway pressure (P_{aw}); mask occlusion pressure ($P_{mask-occl}$) obtained during the use of PS 15 cmH₂O. The air leak around the mask is illustrated by the difference between proximal and distal inspiratory flows. Note the mirror relationship between the P_{aw} and $P_{mask-fit}$ tracings during the inspiratory and expiratory phases. The mask was pushed toward the face when P_{aw} decreased below baseline during the triggering phase, which caused a brief elevation in the $P_{mask-fit}$ and $P_{mask-occl}$. The progressive rise in P_{aw} during the inspiratory phase lifted the mask off the model's face resulting in a drop of $P_{mask-fit}$. Both the rise in the P_{aw} and the drop in the $P_{mask-fit}$ contributed to the steep decline observed in the $P_{mask-occl}$. **B** Waveforms recorded during PS 16 cmH₂O. It is possible to see that all flow delivered by the ventilator was leaked around the mask when the gradient between $P_{mask-fit}$ and P_{aw} approached zero (see also Fig. 3)

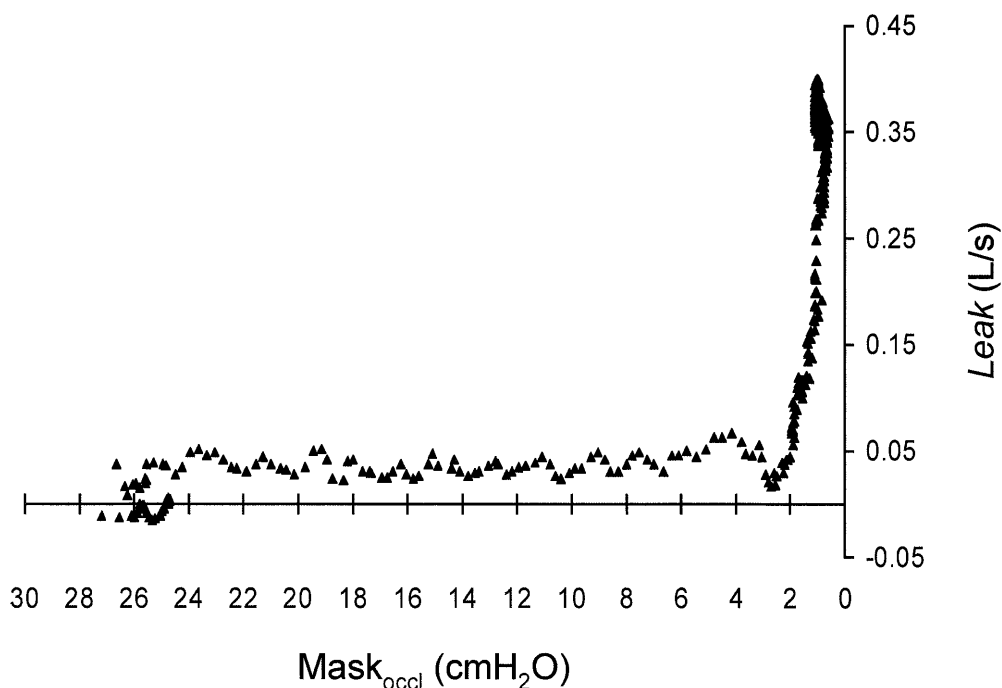
recorded during PS 16 showed that the leak rate was nearly constant and about 0.05 l per second for $P_{mask-occl}$ higher than 2 cmH₂O, and when the $P_{mask-occl}$ fell below 2 cmH₂O, an abrupt increase in the leak rate was observed (Fig. 3).

Discussion

The most important findings of this study can be summarized as follows: (a) mask mechanics, particularly $P_{mask-fit}$ and $P_{mask-occl}$, can be easily measured in cushioned masks, and (b) the dynamics of the air leak around the mask are complex, but an abrupt increase in air leak rate occurs when the gradient between $P_{mask-fit}$ and airway pressure (i.e., $P_{mask-occl}$) approaches zero.

Other authors, using different models, have studied ventilators and modes during simulated NPPV; however, in these models leak occurred through fixed diameter holes placed in the model's circuits, thus the leak rate was defined only by airway pressure and hole resistance [3, 8, 9, 10]. We used a facial mask with a valve that permitted inflation of the mask's low-pressure pneumatic cushion with a known air volume and also allowed recording of pressure variations inside the cushion. The cushion was inflated with 50 ml, a volume necessary to adequately inflate the cushion, but still maintaining the pressure in the cushion lower than 1 cmH₂O before attaching the mask to the mannequin's face. This precau-

Fig. 3 Mask occlusion pressure ($P_{\text{mask-occl}}$) vs. air leak rate around the mask recorded in a breathing cycle during PS 16 cmH_2O . Leak rate was nearly constant and about 0.05 l per second for $P_{\text{mask-occl}}$ higher than 2 cmH_2O , and an abrupt increment in the leak rate was observed when the $P_{\text{mask-occl}}$ fell below 2 cmH_2O . Negative leak rate values (i.e., distal inspiratory flow higher than proximal), at very low magnitude, were recorded during the triggering phase suggesting that small amounts of air entered, through the mask, to the upper airway when the airway pressure was negative



tion was necessary to guarantee that recorded $P_{\text{mask-fit}}$ represented the pressure that fits the mask against the face and not the pressure necessary to inflate the mask's cushion. $P_{\text{mask-fit}}$ was preset at 25 cmH_2O to insure that it was lower than the skin capillary perfusion pressure [11]. Skin damage at the site of mask contact is the most common complication of NPPV, and skin necrosis is normally due to excessive mask fit pressure impairing adequate tissue perfusion [4]. However, no study has systematically described methods of monitoring mask fit pressure. We believe that $P_{\text{mask-fit}}$ is a simple and useful method of guiding mask attachment during NPPV.

The mirror comportment of P_{aw} and $P_{\text{mask-fit}}$, as illustrated in Fig. 2, is fundamental to determining the air leak dynamics, because both the rise in P_{aw} pressure and the drop in $P_{\text{mask-fit}}$ contributed to a decrease in $P_{\text{mask-occl}}$ and facilitated air leak around the mask during inspiration. In the present study only one headgear was tested, but we speculate that for the same proximal airway pressure a small mask displacement, and consequently lower decline in $P_{\text{mask-fit}}$ and $P_{\text{mask-occl}}$, are expected with a headgear consisting of straps with lower elasticity.

In an ideal mask sealing situation, air leak around the mask may not occur if the gradient between $P_{\text{mask-fit}}$ and proximal airway pressure is positive (i.e., $P_{\text{mask-occl}} > 0$). Figure 3 illustrated that a small amount of leak existed even with high levels of $P_{\text{mask-occl}}$, showing that mask sealing was not perfect. The presence of small channels, created by folds in the cushion's membrane and irregularities of the mannequin's face, allowing air passages

to form at the face-mask interface may explain this observed leak pattern. The air leak rate was small and nearly constant for $P_{\text{mask-occl}}$ higher than 2 cmH_2O , however, when $P_{\text{mask-occl}}$ declined below this value, an abrupt increase in the leak rate was noted. It was visually observed that the mask displacement during inspiration was not symmetric, suggesting that $P_{\text{mask-occl}}$ represents the mean of several different mask fit values around the face-mask interface. Probably in some areas the mask was entirely unattached from the face, allowing massive air leak even though the recorded $P_{\text{mask-occl}}$ was positive.

Although pressure support is a spontaneous mode of assisted mechanical ventilation, failure to cycle to exhalation may occur if air leak prevents the inspiratory flow from declining to the preset exhalation trigger [6]. In our study PS 15 cmH_2O , lead to a minimum $P_{\text{mask-occl}}$ of $1.7 \pm 0.1 \text{ cmH}_2\text{O}$. It was the greatest PS level that allowed normal cycling to exhalation. The effective VT ($\text{VT}_{\text{distal}}$) assured by PS 15 cmH_2O was 586 ml (equivalent to 7.8 ml/kg for a 75 kg adult), which we consider satisfactory for most noninvasively ventilated patients. The effects of the use of PEEP on mask mechanics and leak dynamics were not addressed in this experiment, but we have no doubt that the use of PEEP would rise mean and peak inspiratory airway pressures, decreasing $P_{\text{mask-fit}}$ and $P_{\text{mask-occl}}$ and increasing air leak rate. That is why we are convinced that the $P_{\text{mask-fit}}$ should be reset after each change in the PEEP or PS levels.

We believe that these results, although obtained in a mechanical model, illustrate the possibility of monitor-

ing $P_{\text{mask-fit}}$ and $P_{\text{mask-occl}}$. However, clinical studies are necessary to confirm the real benefits of monitoring these parameters during NPPV.

Acknowledgements The authors are indebted to Robert Kacmarek for his helpful comments and suggestions in the preparation of this manuscript.

References

1. Navalesi P, Fanfulla F, Frigerio P, Gregoretti C, Nava S (2000) Physiologic evaluation of noninvasive mechanical ventilation delivered with three types of mask in patients with chronic hypercapnic respiratory failure. *Crit Care Med* 28: 1785–1790
2. Brochard L (2000) What is really important to make noninvasive ventilation work. *Crit Care Med* 28: 2139–2140
3. Hotchkiss JR, Adams AB, Dries DJ, Marini JJ, Crooke PS (2001) Dynamic behavior during noninvasive ventilation. Chaotic support? *Am J Respir Crit Care Med* 163: 374–378
4. Mehta S, Hill NS. Noninvasive ventilation (2001) *Am J Respir Crit Care Med* 163: 540–577
5. Carrey Z, Gottfried SB, Levy RD (1990) Ventilatory muscle support in respiratory failure with nasal positive pressure ventilation. *Chest* 97: 150–158
6. Calderini E, Confalonieri M, Puccio PG, Francavilla N, Stella L, Gregoretti C (1999) Patient-ventilator asynchrony during noninvasive ventilation: the role of expiratory trigger. *Intensive Care Med* 25: 662–667
7. Op't Holt TB, Hall MW, Bass JB, Allison RC (1982) Comparison of changes in airway pressure during continuous positive airway pressure (CPAP) between demand valve and continuous flow devices. *Respir Care* 27: 1200–1209
8. Lofaso F, Brochard L, Hang T, Lorino H, Harf A, Isabey D (1996) Home versus intensive care pressure support devices. Experimental and clinical comparison. *Am J Respir Crit Care Med* 153: 1591–1599
9. Bunburaphong T, Imanaka H, Nishimura M, Hess D, Kacmarek RM (1997) Performance characteristics of bilevel pressure ventilators. A lung model study. *Chest* 111: 1050–1060
10. Smith IE, Shneerson JM (1996) A laboratory comparison of four positive pressure ventilators used in the home. *Eur Respir J* 9: 2410–2415
11. Peerless JR, Davies A, Klein D, Yu D (1999) Skin complications in the intensive care unit. *Clin Chest Med* 20: 453–467